*Proc. of the European Safety and Reliability Conference (ESREL 2026)*
*Edited by* José C. Matos, Paulo B. Lourenço, Michael Beer, Daniel Oliveira, Edoardo Patelli, Hélder S. Sousa, Rui A. Silva and Monica Santamaria

doi: 10.3850/ESREL2026061419_esrel26-p24060-cd

# Operational Reliability Optimization: Integrated Petrochemical Logistics Systems Under Energy Transition via a Multi-Stage Collaborative Framework

Guangtao Fu

*College of Mechanical and Transportation Engineering, China University of Petroleum (Beijing), China. E-mail: fgtao8783@163.com*

Bozhuo Dong

*College of Mechanical and Transportation Engineering, China University of Petroleum (Beijing), China. E-mail: 15174512999@163.com*

Rui Qiu

*College of Mechanical and Transportation Engineering, China University of Petroleum (Beijing), China. E-mail: rqiu@cup.edu.cn*

Renfu Tu

*College of Mechanical and Transportation Engineering, China University of Petroleum (Beijing), China. E-mail: turenfu@foxmail.com*

Haochong Li

*College of Artificial Intelligence, China University of Petroleum (Beijing), China. E-mail: lehoc0401@163.com*

Yongtu Liang*

*College of Mechanical and Transportation Engineering, China University of Petroleum (Beijing), China.*
*Beijing University of Chemical Technology, China. E-mail: liangyt21st@163.com*

The low-carbon transition is fundamentally reshaping the petrochemical industry, exposing integrated petrochemical logistics system to hazards arising from stochastic supply-demand uncertainty and operational vulnerabilities. To mitigate the risks of traditional static planning in this volatile environment, this paper develops the multi-stage collaborative reliability optimization framework. By integrating scenario generation and reduction techniques with stochastic programming, a multi-stage optimization model is established to ensure process safety and handle long-term planning adjustments. Taking a large-scale petrochemical network as a case study, the trade-off between economic expenditure and operational reliability is quantitatively evaluated across four fluctuation scenarios. The research findings demonstrate that the proposed multi-stage model outperforms static model in reliability indicators. Specifically: (i) the multi-stage model achieves a 39.25% reduction in supply failure magnitude, representing a decrease of $18.13 \times 10^4$ tons under the extreme failure scenario, and effectively curtails the average failure duration by 16.82% under high fluctuation scenario; (ii) the service reliability level remains 1.88% higher than that of the static model under extreme fluctuation scenario; and (iii) although the framework necessitates a 9.15% safety premium in objective function value, this investment successfully transforms uncontrollable external hazards into manageable safety margins. These results provide critical decision support for maintaining operational safety and ensuring the continuous reliability of integrated petrochemical systems.

*Keywords*: Petrochemical system, Reliability optimization, Multi-stage collaborative programming, Supply and demand uncertainty, Risk mitigation

## 1. Introduction

The global low-carbon transition is reshaping the petrochemical industry. In the past decade, the global annual demand for refined oil has fluctuated between 900 million and 1.4 billion tons (Liu et al. 2025), the demand for refined oil is expected to peak before 2030 (IEA

2023). Concurrently, demand for methanol and hydrogen exhibits robust growth, projected to dominate 53%~71% of primary energy consumption by 2060 (Popoola, et al. 2026). Consequently, enterprises are compelled to adopt "oil-to-chemicals" strategies. However, the spatial mismatch between the supply and demand for these conversion products necessitates large-scale, cross-regional resource allocation, thereby increasing the vulnerability of the system operation level. The existing supply-demand networks of refined oil and the logistics flows of conversion products are characterized by a high degree of spatial congruence, establishing the physical basis for an integrated petrochemical logistics system (IPLS). However, this structural interdependency ultimately magnifies the risk of systemic cascading failures under operational stress. In actual operation, the IPLS frequently faces severe disruption risks triggered by external extreme events, such as geopolitical conflicts and natural disasters, which critically compromise the overall operational safety and continuous supply reliability of the energy network.

Traditional static planning strategies frequently lead to critical system failures in practice, as their deterministic nature renders them highly vulnerable to dynamic external disturbances and operational disruptions. To mitigate the inherent risks associated with this operational vulnerability, multi-stage planning frameworks have been increasingly adopted as a robust mathematical tool for quantitative risk management and reliability optimization. For instance, Li et al. (2023) addressed the complex risk coupling between chemical production and subsequent supply operations by proposing a multi-time-domain optimization framework. Similarly, Fattahi et al. (2020) developed a data-driven multi-stage planning method focused on designing highly reliable distribution networks under severe disruption risks, thereby validating the strategy's effectiveness in systemic risk mitigation and operational recovery. Consequently, these studies substantiate the paramount role of multi-stage planning, functioning not merely as an economic optimization technique but as an essential safety mechanism for dynamically calibrating operating parameters to ensure the continuous reliability of complex systems.

Critical vulnerabilities within IPLS from highly volatile demands for refined oil and conversion products, coupled with unpredictable external disruption risks. To mathematically quantify and mitigate these hazards, the stochastic programming strategy based on scenario generation and reduction serves as an essential framework, striking an effective balance between traditional probabilistic risk assessment and robust safety optimization. This strategy has been effectively applied in various complex energy logistics cases. For instance, Zeng et al. (2020) utilized scenario reduction techniques to optimize the risk-informed operation of renewable energy systems, verifying the capacity of the reduced scenario sets to preserve critical statistical features. Furthermore, Gao et al. (2024) integrated principal component analysis with the K-medoids clustering algorithm to extract typical and high-consequence failure scenarios from massive historical datasets, providing precise safety boundary conditions for the fault-tolerant operation of integrated energy systems. Overall, this scenario-based risk management strategy empowers decision-makers to formulate high-quality resource allocation plans that guarantee continuous supply reliability during unnormal operations while establishing robust fault tolerance against severe external shocks.

However, when existing studies apply multi-stage planning frameworks, their optimization objectives are predominantly restricted to the immediate response of a single logistics system. This narrow focus overlooks the complex, risk-informed trade-offs between operational cost efficiency and long-term continuous system reliability. By ignoring systemic vulnerabilities and the critical need for fault tolerance under the uncertain and hazard-prone environment of the global energy transition, traditional models fail to adequately prevent cascading failures. Consequently, there remains a pressing need for a comprehensive mathematical framework capable of dynamically balancing proactive risk mitigation with operational safety across IPLS.

## 2. Methodology

### 2.1. *Problem description*

As illustrated in Figure 1, integrated petrochemical logistics system comprises four interdependent critical sub-systems: supply, transfer, transportation, and demand. Both refineries and depots are equipped with storage facilities that function explicitly as risk mitigation buffers, designed to absorb disruption shocks. These sub-systems are tightly coupled through four transportation modes (pipeline, waterway, railway, and highway), constituting a highly complex critical infrastructure network. While this tight coupling facilitates the efficient flow of materials, it simultaneously magnifies the system's inherent vulnerability to cascading failures. Furthermore, refineries operate as supply nodes with the production flexibility to convert refined oil into diverse chemical products (e.g., methanol, liquid ammonia, hydrogen, ethylene glycol). Within the context of system safety, this conversion capability acts as a crucial fault-tolerance mechanism, allowing operators to dynamically reconfigure process pathways under severe interference. During actual operation, this integrated network is continuously exposed to stochastic environmental hazards and unpredictable external disruption risks. These uncertainties manifest as extreme fluctuations in supply and demand, continuously challenging the operational safety margins and operational reliability of the entire petrochemical system.

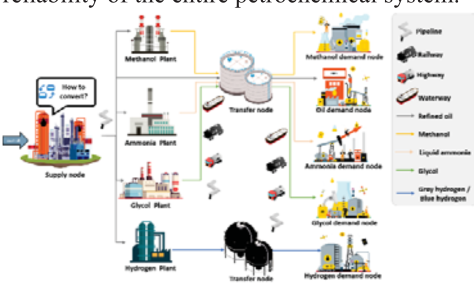


Fig. 1. The integrated petrochemical logistics system of refined oil and conversion products.

## 2.2. *Research framework*

Figure 2 illustrates the multi-stage collaborative reliability optimization framework designed to ensure the operational safety and continuous reliability of the integrated petrochemical network. The architecture comprises three modules. Module 1 utilizes Monte Carlo stochastic simulation to generate a large-scale set of hazard scenarios. By defining specific fluctuation boundaries, this module mathematically captures the non-linear characteristics of operational uncertainties and severe disruption risks. Module 2 serves as the computational core for systemic operational risk mitigation. It involves two critical stages: first, it builds a multi-stage collaborative optimization model based on multi-stage planning strategies to deal with plan adjustments in long time dimensions. Second, it introduces the K-means clustering algorithm for scenario reduction, accurately extracting typical and extreme scenarios from large-scale scenarios by combining multi-dimensional evaluation indicators. Finally, Module 3 executes a system risk evaluation. By replacing traditional metrics with a multi-dimensional system explicitly focused on system reliability, risk mitigation and economics. Furthermore, through a real-world petrochemical case study, it demonstrates how the proposed multi-stage model vastly outperforms static model, thereby providing quantitative decision support for ensuring system safety and highly reliable actual operations.

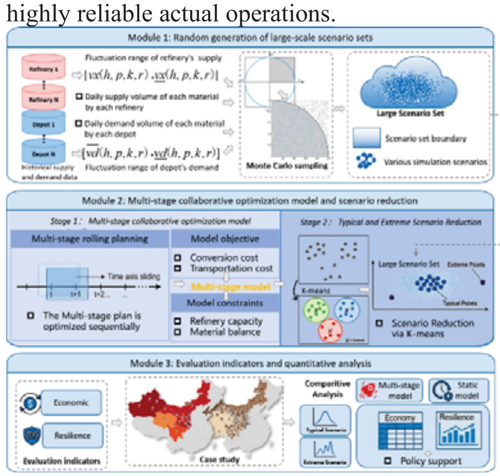


Fig. 2. The multi-stage collaborative reliability optimization framework for integrated comprehensive logistics system.

## 2.3. *Optimization model*

### 2.3.1. *Objective function*

The multi-stage collaborative optimization model aims to reduce the total cost of the three segments of transportation, conversion, and storage in the integrated comprehensive logistics system. Eq.(1) represents the objective function $TOC$, which includes average transportation cost $E_{h \in H}(TRC_h)$, average conversion cost $E_{h \in H}(CON_h)$, average storage cost $E_{h\in H}(STC_h)$, and average stockout penalty cost $E_{h\in H}(PEC_h)$.

$$\begin{aligned} &min\,TOC \\ &= E_{h\in H}(TRC_h + CON_h + STC_h + PEC_h) \\ &= \sum_{h\in H} \varphi_h (TRC_h + CON_h + STC_h + PEC_h) \end{aligned} \tag{1}$$

### 2.3.2. *Refinery operational constraints*

The refined oil and converted product planned production volume $VX_{h,p,k,r}$ at these refineries is equal to the planned production sampling volume $\widetilde{VX}_{h,p,k,r}$ in scenario $h$. Furthermore, the inventory volume $VU_{h,p,k,r}$ is constrained to remain within its predefined operational safety boundaries, bounded by the minimum inventory volume $vu_{k,r}^{\min}$ and maximum inventory volume $vu_{k,r}^{\max}$.

Eq.(2) represents the constraint for the transfer-out of refined oil products in each scenario $h$. The refined oil supply volume $VR_{h,p,k,r}$, plus the cumulative sum of refined oil transfer-out volume $\sum_{r'\in G} VC_{h,p,k,r,r'}$, minus the refined oil planned production volume $VX_{h,p,k,r}$. Eq.(3) represents the constraint for the transfer-in of conversion products in each scenario $h$. The converted product supply volume $VR_{h,p,k,r}$, minus the cumulative sum of converted product transfer-in volume $\sum_{r'\in O} \gamma_{k,r',r} \cdot VC_{h,p,k,r',r}$, plus the converted product planned production volume $VX_{h,p,k,r}$.

$$\begin{aligned} VR_{h,p,k,r} + \sum_{r'\in G} VC_{h,p,k,r,r'} \le VX_{h,p,k,r} \\ \forall h\in H, p\in P_{win}, k\in S, r\in O \end{aligned} \tag{2}$$

$$\begin{aligned} VR_{h,p,k,r} \le \sum_{r'\in O} \gamma_{k,r',r} \cdot VC_{h,p,k,r',r} + VX_{h,p,k,r} \\ \forall h\in H, p\in P_{win}, k\in S, r\in G \end{aligned} \tag{3}$$

### 2.3.3. *Transfer capacity constraint*

Eq.(6) ensures that the transportation volume $\sum_{k'\in T\cup D}\sum_{r\in R} VT_{h,p,k,k',z,r}$ from a refinery or transit depot using transportation modes within unit time period is less than the maximum sending capacity $vf_{k,z}^{\max}$ in scenario $h$.

There are constraints on the volume received by regular depots or transit depots via different transportation modes within unit time period (Zhang et al. 2025). Eq.(4) ensures that the sum of the received volume $\sum_{k'\in S\cup T}\sum_{r\in R} VT_{h,t,k',k,z,r}$ from refineries and transit depots and the in-transit transportation volume $\sum_{k''\in S\cup T}\sum_{r\in R} VTZ_{h,p,k'',k,z,r}$ at the planning cutoff is less than the depot's maximum receiving capacity $vs_{k,z}^{max}$ in scenario $h$.

$$\begin{aligned} &\sum_{k'\in S\cup T}\sum_{r\in R} VT_{h,t,k',k,z,r} \\ &+ \sum_{k''\in S\cup T}\sum_{r\in R} VTZ_{h,p,k'',k,z,r} \le vs_{k,z}^{max} \\ &\forall h\in H, p\in P_{win}, k\in T\cup D, z\in Z \end{aligned} \tag{4}$$

### 2.3.4. *Depot capacity constraint*

Eq.(5) ensures that the demand volume $VD_{h,p,k,r}$ at these depots is equal to the demand sampling volume $\widetilde{VD}_{h,p,k,r}$ in scenario $h$. Furthermore, the refined oil inventory volume $VU_{h,p,k,r}$ at these depots does not exceed the maximum inventory volume $vu_{k,r}^{\max}$ and is not less than the minimum inventory volume $vu_{k,r}^{\min}$ in scenario $h$.

$$\begin{aligned} VD_{h,p,k,r} = \widetilde{VD}_{h,p,k,r} \\ \forall h\in H, p\in P_{win}, k\in T\cup D, r\in R \end{aligned} \tag{5}$$

### 2.3.5. *Material balance constraint*

At the initial time, the inventory volume of each refinery $VU_{h,p=0,k,r}$ is equal to its initial inventory volume $uu_{k,r}$. The inventory volume $VU_{h,p+1,k,r}$ at time period $p+1$, equals the inventory volume $VU_{h,p,k,r}$ at time point $p$, plus the supply volume $VR_{h,p,k,r}$ at time period $p$, minus the transportation volume $\sum_{k'\in T\cup D}\sum_{z\in Z} VT_{h,p,k,k',z,r}$ at time period $p$.

$$\begin{aligned} VU_{h,p+1,k,r} = VU_{h,p,k,r} + VR_{h,p,k,r} \\ - \sum_{k'\in T\cup D}\sum_{z\in Z} VT_{h,p,k,k',z,r} \\ \forall h\in H, p\in P_{win}, k\in S, r\in R \end{aligned} \tag{6}$$

At the initial time, the average inventory volume of each depot $VU_{h,p=0,k,r}$ is equal to the depot's initial inventory volume $uu_{k,r}$. At time period $p+1$, the average inventory volume $VU_{h,p+1,k,r}$ equals the sum of the average inventory volume $VU_{h,p,k,r}$, the average stockout volume $VQ_{h,p,k,r}$, the receiving volume $\sum_{k'\in S\cup T}\sum_{z\in Z} V_{h,p,k',k,z,r}^{T}$, and in-transit transportation volume $\sum_{k''\in S\cup T}\sum_{z\in Z} VTZ_{h,p,k'',k,z,r}$, minus sending volume $\sum_{k'''\in T\cup D}\sum_{z\in Z} VT_{h,p,k,k''',z,r}$ and the average demand volume $VD_{h,p,k,r}$ at time period $p$.

$$\begin{aligned} VU_{h,p+1,k,r} &= VU_{h,p,k,r} + VQ_{h,p,k,r} \\ &+ \textstyle\sum_{k' \in S \cup T} \sum_{z \in Z} VT_{h,p,k',k,z,r} \\ &+ \textstyle\sum_{k'' \in S \cup T} \sum_{z \in Z} VTZ_{h,p,k'',k,z,r} \\ &- \textstyle\sum_{k''' \in T \cup D} \sum_{z \in Z} VT_{h,p,k,k''',z,r} \\ &- VD_{h,p,k,r} \ \forall h \in H, \in P_{win}, k \in S, r \in R \end{aligned} \tag{7}$$

### 2.4. *Scenario generation and reduction model*

#### 2.4.1. *Scenario generation model*

Based on the supply and demand fluctuation intervals obtained from a prediction algorithm, Eq.(14)~(17) assume that the planned supply, denoted as the random variable $\widetilde{VX}_{h,p,k,r}$, follows a distribution centered around the daily planned supply $\varepsilon_{p,k,r}$ with a fluctuation interval of $\delta_{h,p,k,r}$. Similarly, planned demand $\widetilde{VD}_{h,p,k,r}$ fluctuates within $\lambda_{h,p,k,r}$ around the baseline $\varepsilon_{p,k,r}$ (Ryou, et al. 2026).

$$\widetilde{VX}_{h,p,k,r} = \varepsilon_{p,k,r} + \delta_{h,p,k,r} \quad \forall h \in H, p \in P, k \in S, r \in R \tag{8}$$

$$\widetilde{VD}_{h,p,k,r} = \varepsilon_{p,k,r} + \lambda_{h,p,k,r} \quad \forall h \in H, p \in P, k \in D, r \in R \tag{9}$$

#### 2.4.2. *Scenario reduction model*

K-means clustering is employed to select a set of representative scenarios from the large-scale scenario optimization results. After the optimization model is solved for all generated scenarios $h$, the evaluation results for various metrics are obtained for each scenario. We let $I_{h,j}$ denote the value of evaluation metric $j$ for scenario $h$. Let $J = \{1,2,\ldots,j_{max}\}$ denote the set of all indicators, indexed by $j$.

$$I_{h,j} = [Econ_h, Env_h, Ener_h, Res_h] \quad \forall h \in H, j \in J \tag{10}$$

To eliminate the influence of different units and magnitudes across the various metrics, Z-score standardization is applied to construct a standardized vector $\hat{I}_{h,j}$. In this equation, $\mu_j$ and $\sigma_j$ represent the mean and standard deviation, respectively, of evaluation metric $j$ across all scenarios.

Based on the similarity of these standardized metrics, the algorithm partitions the scenario set $S$ into $C$ distinct clusters, such that $S = \sum_{c \in C} S_c$. From each cluster, a typical and an extreme scenario are selected. The typical scenario $s_c^{typ}$ is the one that minimizes the sum of squared distances to the cluster's centroid for all evaluation metrics j. Conversely, the extreme scenario $s_c^{ext}$ as the one that maximizes this sum of squared distances. Here, $\Phi_{c,j}$ denotes the centroid of metric $j$ for cluster $c$.

### 2.5. *Indicator construction*

Beyond basic physical routing, the fundamental objective of the integrated network is to proactively mitigate stochastic supply-demand disruption risks and guarantee operational safety alongside continuous service reliability. Consequently, multi-dimensional evaluation indicators are required to rigorously evaluate system vulnerabilities. This paper proposes three core reliability and fault-tolerance indicators: magnitude of supply failure average failure duration, and service reliability level. Economic evaluation indicators are used to quantify costs including conversion, transportation, storage, and penalty.

#### 2.5.1. *Supply failure magnitude (SFM)*

This vulnerability indicator quantifies the absolute structural magnitude of unmet demand.

$$VY_{h,p,k,r} = \sum_{k' \in S \cup T} \sum_{z \in Z} VT_{h,p,k',k,z,r} + VU_{h,p,k,r} \tag{11}$$

$$SFM_h = \sum_{p \in P_{win}} \sum_{k \in T \cup D} \sum_{r \in R} \max\{0, VD_{h,p,k,r} - VY_{h,p,k,r}\} \tag{12}$$

#### 2.5.2. *Average failure duration (AFD)*

This temporal risk indicator measures the recovery latency and the overall operational downtime of the degraded system following a disruption.

$$VF_{h,p,k,r} = \sum_{k' \in S \cup T} \sum_{z \in Z} VT_{h,p,k',k,z,r} + VU_{h,p,k,r} - VD_{h,p,k,r} \tag{13}$$

$$RS_h = \begin{cases} 1, if(VF_{h,p,k,r} < 0) \\ 0, if(VF_{h,p,k,r} \geq 0) \end{cases} \tag{14}$$

$$AFM_h = \frac{\sum_{p \in P_{win}} \sum_{k \in T \cup D} \sum_{r \in R} RS_h}{K} \tag{15}$$

#### 2.5.3. *Service reliability level (SRL)*

This critical metric measures the operational integrity of the system, verifying the extent to which the optimization framework has successfully achieved fault-tolerant matching under severe environmental stress.

$$SRL_h = \frac{\sum_{p\in P_{win}} \sum_{k\in T\cup D} \sum_{r\in R} \frac{VD_{h,p,k,r}-SFM_h}{VD_{h,p,k,r}}}{K} \quad (16)$$

## 3. Case study

This paper takes the integrated comprehensive logistics system of a petrochemical enterprise in China as a case for study. The case involves 20 materials (O01-O20), among which 15 materials are traditional refined oils, covering different types of diesel (O01-O07) and different types of gasoline (O08-O15), and 5 materials are chemical and clean energy converted products, including ethylene glycol (O16), methanol (O17), grey hydrogen (O18), blue hydrogen (O19), and liquid ammonia (O20). Figure 3(a) shows the distribution locations of 16 supply nodes (S1-S16), and Figure 3(b) shows the distribution locations of 11 transit nodes (T1-T11) and 80 demand nodes (D1-D80). Each supply node has refined oil supply capability and conversion capability. Demand nodes are divided into refined oil demand nodes and refined oil and converted product demand nodes. The monthly supply and demand in each region are indicated by colour shading, and the geographical mismatch between supply and demand of various products requires the use of 3 transportation modes for resource allocation.

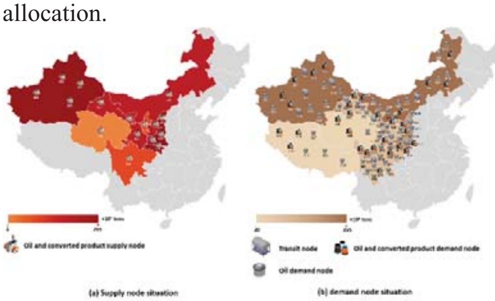

Fig. 3. Schematic diagram of the system node distribution.

Table 1 summarizes the material conversion ratios based on the element conservation method (Tong et al. 2013), taking converting O01 into O16 as an example, where consuming 1 ton of O01 gets 0.49 tons of O16. Table 2 summarizes the unit transportation costs of four transportation modes. Considering policy subsidies, equipment depreciation, actual operation, etc., it is assumed that the unit conversion cost is 2100 CNY/t, the warehouse unit inventory cost is 10 CNY/t, and the unit penalty cost t is $1\times10^5$ CNY/t.

Table 1. Conversion ratios among various materials.

| Transfer-in material | Transfer-out materials | Ratio |
|---|---|---|
| O01-O07 | O16 | 0.49 |
| | O17 | 2.29 |
| | O18 | 0.2 |
| | O19 | 0.2 |
| | O20 | 1.13 |
| O08-O15 | O16 | 0.73 |
| | O17 | 2.27 |
| | O18 | 0.2 |
| | O19 | 0.2 |
| | O20 | 1.13 |

Table 2. Transportation cost of different transportation modes.

| Mode | Transportation cost (CNY/t-km) |
|---|---|
| TRK | 0.68 |
| PIP | 0.15 |
| RAL | 0.30 |

## 4. Results and discussion

### 4.1. *Scenario reduction*

To ensure the optimization model can fully capture the uncertainty of the system, the number of scenarios needs to be determined. In the figure 4 of the objective function value, when the scenario set reaches 830 scenarios, the objective function begins to show stability. Therefore, this study finally generated 830 scenarios and selected two typical and two extreme scenarios from them for detailed analysis later. Table 2 summarizes the four scenarios. Furthermore, this paper applies the traditional deterministic logistics model (TDLM) and the multi-stage optimization model (MAOM) to four scenarios.

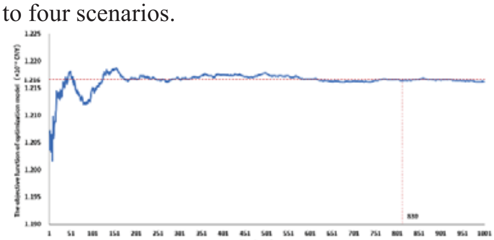

Fig. 4. Convergence curves of the model objective function with respect to the number of scenarios.

Table 2. Characteristics of operational risk and supply-demand fluctuation scenarios.

| Scenario | Description |
|---|---|
| Slight Fluctuation (SFS) | Minor supply-demand adjustments |
| Moderate Fluctuation (MFS) | Recognizable deviations from the mean |
| High Fluctuation (HFS) | Substantial structural oscillations |
| Extreme Fluctuation (EFS) | Unpredictable surges or sharp drops |

### 4.2. *Indicator analysis*

Figure 5 presents a comparative reliability analysis between the static model and the proposed multi-stage model across four fluctuation scenarios. As the severity of operational hazards intensifies from the slight fluctuation scenario to the extreme fluctuation scenario, the fault tolerance of the multi-stage model becomes increasingly pronounced. The service reliability level of the static model demonstrates significant vulnerability to increasing volatility, deteriorating from 95.96% down to 95.23%, which signifies a heightened risk of system-wide failure. In contrast, while the multi-stage model also experiences environmental stress, it maintains a robust and highly service reliability level between 97.10% and 97.93%. Under extreme fluctuation scenario, the multi-stage model achieves a service reliability level 1.88% higher than the static model, effectively preventing supply-chain breakdowns. From the perspective of the objective function, the static model maintains a deceptively low-cost baseline of approximately $12.01\times10^{9}$ CNY by neglecting the safety margins. Conversely, the multi-stage model's risk-weighted expenditure increases alongside the hazard level, peaking at $13.01\times10^{9}$ CNY in the extreme fluctuation scenario. Although this represents a 9.15% increase in operational expenditure, this surplus is mathematically characterized as a "safety premium", which serves as a necessary investment to reinforce the system's structural reliability and proactively buffer against catastrophic uncertainty shocks.

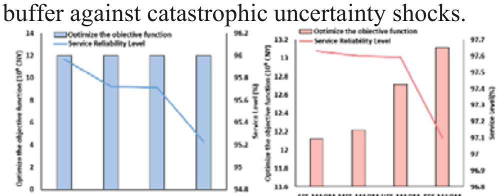


Fig. 5. Comparative analysis of service reliability level and objective function.

Figure 6 illustrates a comparative supply failure magnitude and average failure duration under varying disruption intensities. For the static model, as the system hazard escalates from slight fluctuation scenario to extreme fluctuation scenario, the supply failure magnitude demonstrates an upward trend, peaking at $46.29\times10^{4}$ t in the extreme fluctuation scenario. In contrast, the multi-stage model effectively constrains the supply failure magnitude to $28.06\times10^{4}$ t, representing a substantial reduction of $18.13\times10^{4}$ t and a corresponding 39.25% decrease compared to the static model. Across all fluctuation scenarios, the average failure duration of the multi-stage model remains consistently lower than that of the static model. Specifically, under high fluctuation scenario, the multi-stage model successfully shortens the average failure duration from 4.94 days to 4.11 days, representing a 16.82% improvement in operational recovery speed. These results quantitatively demonstrate that the proposed framework serves as a robust fault-tolerant mechanism, enabling the integrated system to more rapidly mitigate operational failures and restore process safety following severe supply-demand shocks.

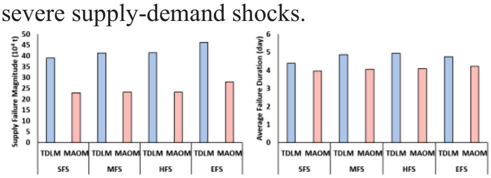


Fig. 6. Comparative analysis of supply failure magnitude and average failure duration.

## 5. Conclusions

Driven by the systemic risks of the energy transition and stochastic supply-demand fluctuations, traditional static planning proves inadequate in mitigating operational vulnerabilities within integrated petrochemical logistics system. This study establishes a multi-stage collaborative reliability optimization framework that serves as a mathematical tool to quantitatively evaluate operational reliability, risk mitigation and economics, across varying degrees of operational uncertainty.

The research findings demonstrate that the proposed multi-stage model significantly outperforms static model in reliability indicators. Under the extreme fluctuation scenario, the supply failure magnitude is reduced by $18.13\times10^{4}$ tons, an improvement of 39.25%. Regarding the system's operational recovery, the multi-stage model achieves a superior response speed. The average failure duration decreases from 4.94 days to 4.11 days in high fluctuation scenario, marking a 16.82% reduction in operational downtime. Furthermore, the service reliability level remains 1.88% higher than that of the static model under extreme fluctuation scenario. From a risk mitigation perspective, while the multi-stage model necessitates a 9.15% increase in the objective function value, this expenditure is characterized as a necessary "safety premium". This strategic investment successfully transforms volatile external hazards into manageable safety margins, thereby significantly enhancing the overall operational safety and structural reliability of the integrated petrochemical system.

**Acknowledgement**

This work is supported by the National Natural Science Foundation of China (52502411), National Key Research and Development Program(2024YFE0100800). The authors are grateful to all study participants.

**Appendix A. Nomenclature**

| Decision variables | |
|---|---|
| $VT_{h,p,k,k\prime,z,r}$ | Transportation volume of product $r$ sent from node $k$ to node $k'$ by transportation mode $z$ at time period $p$ in scenario $h$, t |
| $VTZ_{h,p,k,k\prime,z,r}$ | In-transit transportation volume of product $r$ sent from node $k$ to node $k'$ by transportation mode $z$ at time period $p$ in scenario $h$, t |
| $VX_{h,p,k,r}$ | Planned production volume of product $r$ in node $k$ at time period $p$ in scenario $h$, t |
| $\widetilde{VX}_{h,p,k,r}$ | Planned production sampling volume of product $r$ in node $k$ at time period $p$ in scenario $h$, t |
| $VR_{h,p,k,r}$ | Supply volume of product $r$ in node $k$ at time period $p$ in scenario $h$, t |
| $VC_{h,p,k,r,r\prime}$ | Transfer-out\ transfer-in volume of oil $r$ to oil $r'$ in refinery $k$ at time period$p$ in scenario $h$, t |
| $VU_{h,p,k,r}$ | Inventory volume of product $r$ in node $k$ at time point $p$ in scenario $h$, t |
| $VQ_{h,p,k,r}$ | Stockout volume of product $r$ in node $k$ at time point $p$ in scenario $h$, t |
| $VD_{h,p,k,r}$ | Demand volume of product $r$ in node $k$ at time period $p$ in scenario $h$, t |
| $\widetilde{VD}_{h,p,k,r}$ | Demand sampling volume of product $r$ in node $k$ at time period $p$ in scenario $h$, t |

**References**

Fattahi M, Govindan K (2020). Data - Driven Rolling Horizon Approach for Dynamic Design of Supply Chain Distribution Networks under Disruption and Demand Uncertainty. Decision Sciences, 53(1): 150-180.

Gao B, Zhu Y, Li Y (2024). Optimal Operation Strategy Analysis with Scenario Generation Method Based on Principal Component Analysis, Density Canopy, and K-medoids for Integrated Energy Systems. Journal of Modern Power Systems and Clean Energy, 12(1): 89-100.

IEA (2023). World Energy Outlook 2023.

Li H, Zhang S, Qiu T (2023). Receding Horizon Optimization of Ethylene Cracking Operation and Scheduling under Supply Chain Fluctuations. Industrial & Engineering Chemistry Research, 2023, 62(12): 5125-5140.

Liu J, Guo F, Shi Y, et al. (2025). Study on the evolutionary characteristics and robustness of the global refined oil trade network. Energy, 331: 137032.

Mucci S, Bongartz D (2025). Feature-based scenario clustering and selective degrees of freedom reduction for two-stage stochastic optimization of Power-to-Methanol. Chemical Engineering Research and Design, 223: 311-330.

Popoola L T, Nwogbu C C, Taura U, et al. (2026). Achieving effective operations in petrochemical industries using affordable and clean energy: Techniques, benefits, barriers and solutions. Cleaner Waste Systems, 13: 100453.

Ryou H S, Kim S H, Lee H S, et al. (2026). A multi-path time-series generation and prediction model for financial markets using discriminator-filtered Monte Carlo TimeGAN. Applied Soft Computing, 186: 114106.

Tong K, Gong J, Yue D, et al. (2013). Stochastic Programming Approach to Optimal Design and Operations of Integrated Hydrocarbon Biofuel and Petroleum Supply Chains. ACS Sustainable Chemistry & Engineering, 2(1): 49-61.

Zeng Y, Li C, Wang H (2020). Scenario-Set-Based Economic Dispatch of Power System With Wind Power and Energy Storage System. IEEE Access, 8: 109105-109119.

Zhang X, Fu G T, Liao Q, et al. (2025). Large-scale hydrogen supply chain vision with blended pipeline transportation of China. Renewable Energy, 240: 122230.